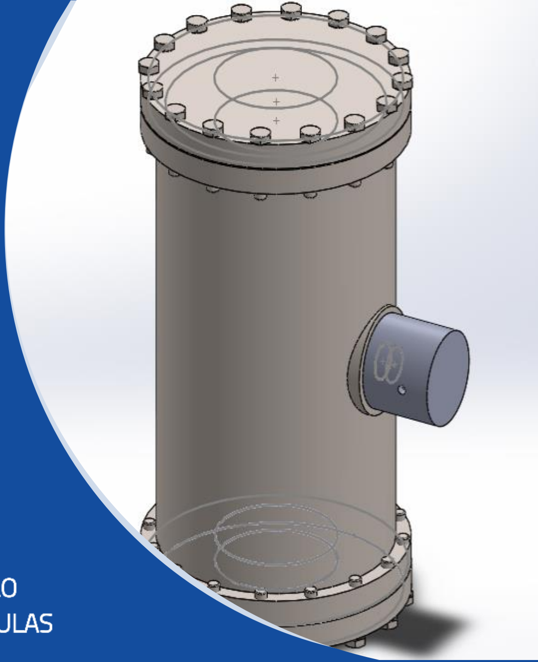

LABORATÓRIO DE INSTRUMENTAÇÃO E FÍSICA EXPERIMENTAL DE PARTÍCULAS

partículas e tecnologia

Dual-Stage Gas Proportional Scintillation Counter – New Developments

A.F.V. Cortez, C.A.N. Conde, S.J.C. do Carmo, F.I.G.M. Borges

Contact: andre.cortez@coimbra.lip.pt

Pisa Meeting on Advanced Detectors 2018, May 27- June 2, 2018 - Isola d'Elba (Italy)

Contents

Objectives and Motivation

Develop a new high-pressure, xenon-based gaseous radiation detector of the GPSC type for hard X-ray and gamma-ray spectrometry.

Here are some reasons why use **HPXe GPSC**?

*Energy resolution;

*Operation at room temperature;

*Lower cost;

*Large detection area;

*Flexibility in the geometry definition;

1.

Gas Proportional Scintillation Counter – The Detector

The Detector – MGHP GPSC

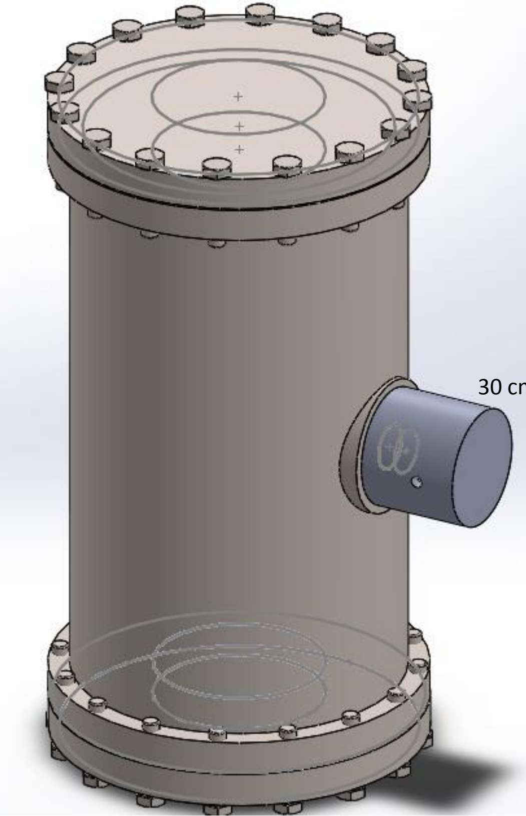

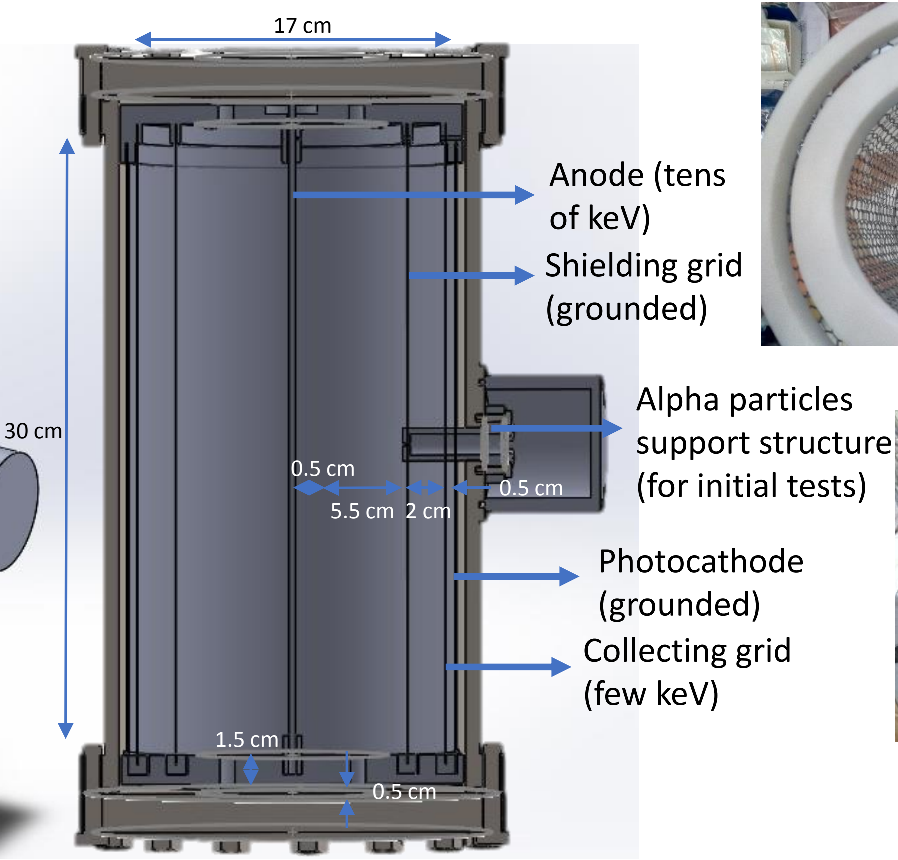

Working Principle
Signal Formation

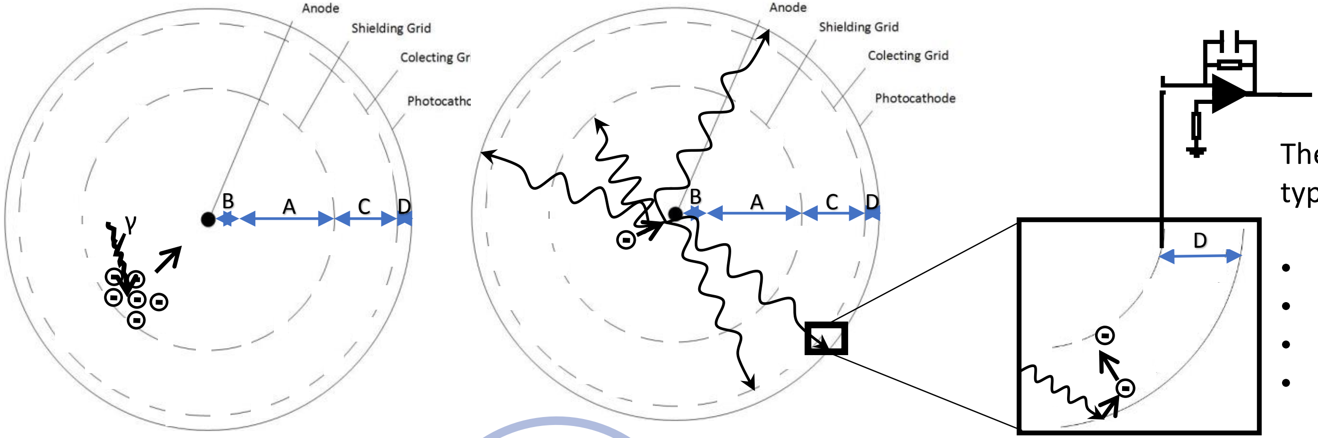

The HPXe detectors of the MGHP-GPSC type consist of four distinct regions:

- **A** - Absorption/Drift Region;
- **B** - Secondary Scintillation Region;
- **C** - Electric Field Barrier Region;
- **D** - Photoelectron Collecting Region;

Region A

Photon

Energy deposition

- Incident energy (Er)
- w-value
- Gas

Charge

Region B

Amplification

- E/p at the anode
- Pressure
- Gas

VUV photon

Region D

Charge

Collection

- Solid angle
- Opt. Transmission
- Quantum Efficiency
- Extraction Efficiency (η)

$$Gain = N_S . T_{opt} . QE . \eta$$

T_{opt} - Grids optical transm.
QE- Quantum Efficiency
η - Extract. Efficiency

$$T_{opt} = T_{shield} . T_{collect.}$$

$$N_S = \iint \underbrace{(AE_S(r) - pB)}_{\text{Photon production}} \underbrace{\left(\frac{2\pi - 2\theta(r)}{2\pi}\right)}_{\text{Anode shadow}} \underbrace{\frac{\Omega(r,z)}{4\pi}}_{\text{Solid angle}} dr\, dz$$

Photon production Anode shadow Solid angle

Planar vs Cylindrical Geometry

Energy Range: 100 keV – 1 MeV

Regions	E/p $V.cm^{-1}torr^{-1}$	Length Cylindrical	Length Planar
Absorption/Drift	0,03<1	30x5,4 cm	4,0 cm
Scintillation	1 – 6	0,5 cm	0,7 cm
Optical transmission	-	-	1,2 cm
Electric field barrier	-	2,0 cm	2,4 cm
Photoelectron collection	<1	0,5 cm	1 cm

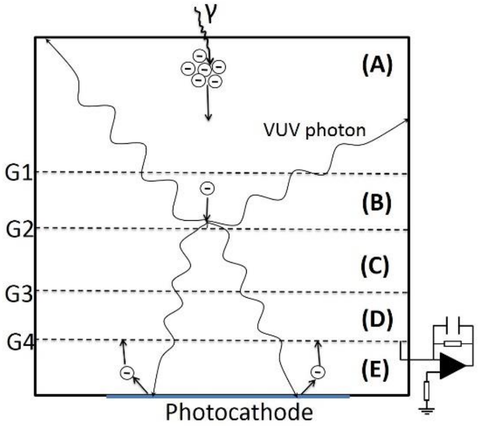

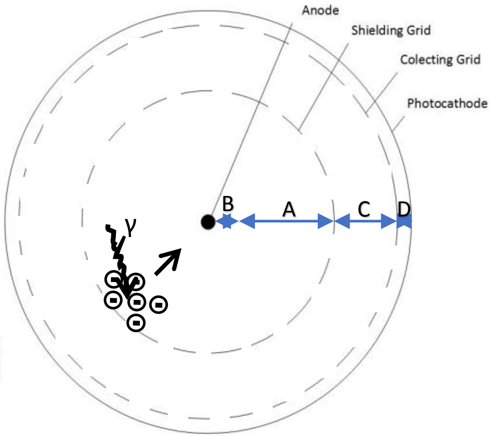

Characteristics	Cylindrical geometry (Planar)
Pressure Range	<20 atm (<10 atm)
Detect. Efficiency (662 keV/15 atm)	~20% (<4%)
Solid Angle (Ω/4π)	0,48-0,87 (0,12)
Detector Active Volume	3369 cm^3 (726 cm^3)
Detector gain	10 - 30 phe-/e- (~10 phe-/e-)

Comparing both geometries, the cylindrical presents:

- Improved Solid Angle
- Improved Detect. Efficiency
- Improved Active Volume of Detection
- Optical Transmission
- Lower Biasing Voltage for the same gain

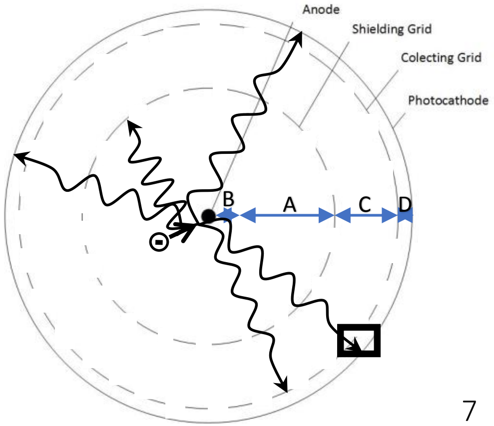

2.

Simulation and Experimental Results

LIP

Tests with Alpha Particles - Simulation

Energy of the ^{241}Am – 5.486 MeV

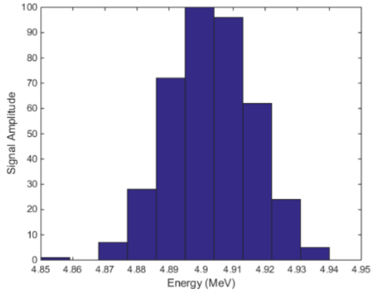

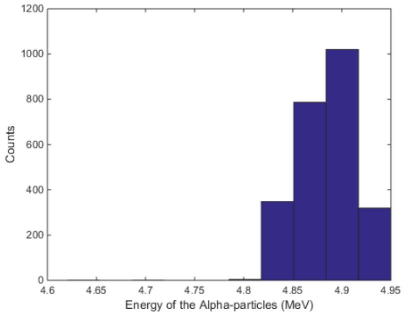

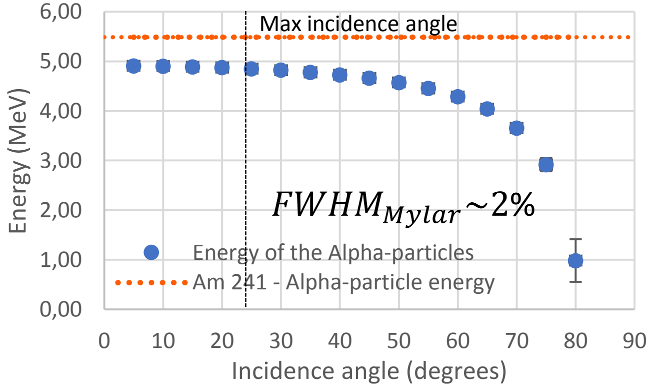

Combined effect of about 2% in the energy dispersion

+

Energy degradation

Deterioration due to the Mylar window

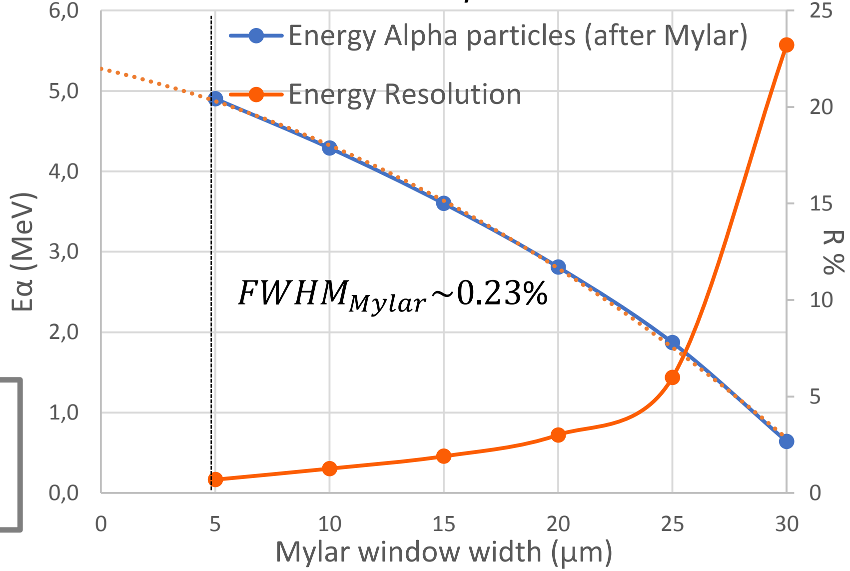

Alpha particles end up with only **4.486 MeV** after crossing the Mylar window **+ energy dispersion.**

Experimental Tests with Alpha Particles

Signal

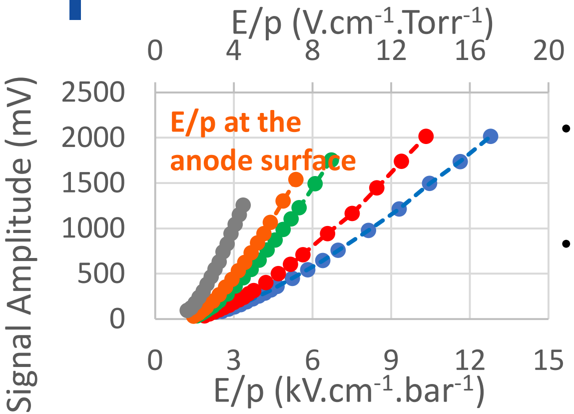

- Scintillation above 2 V.cm-1.Torr-1 at the anode
- Positive feedback observed above 1 V.cm-1.Torr-1

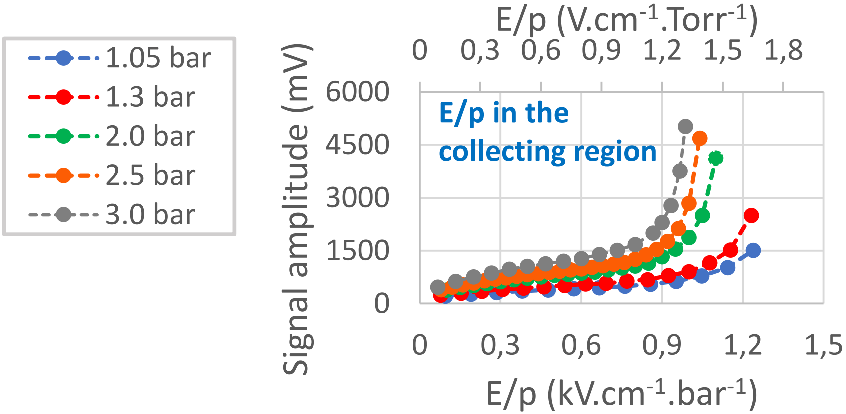

E/p anode

- Extended scintillation region (**small ionization** due to the **radial electric field**)

E/p collecting region

- Positive feedback in the collect. region
- Increasing extraction efficiency

Signal increases (more light being produced) → **Improves greatly the gain**

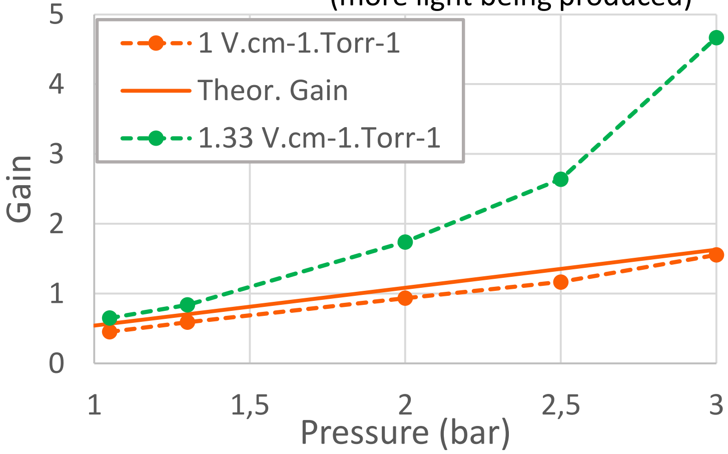

Experimental Tests with Alpha Particles

Energy Resolution vs E/p

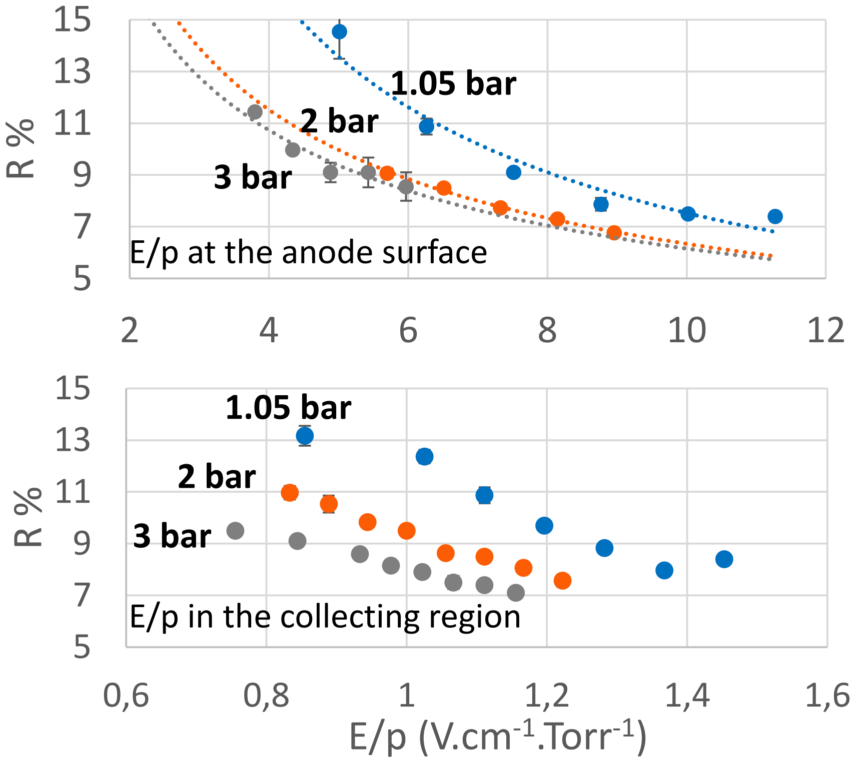

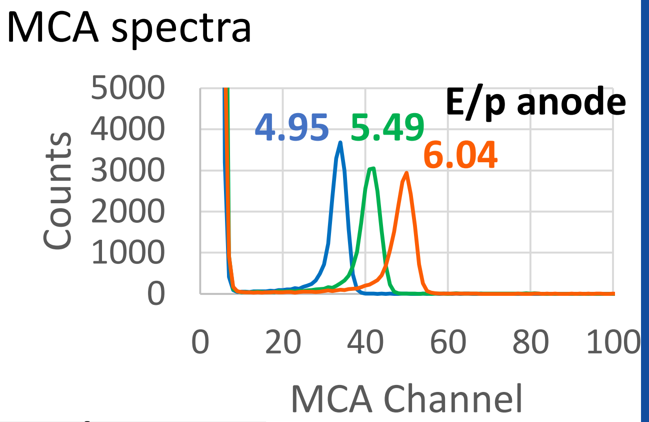

- **R%** improves **with E/p** at the **anode** surface **above ionization threshold**

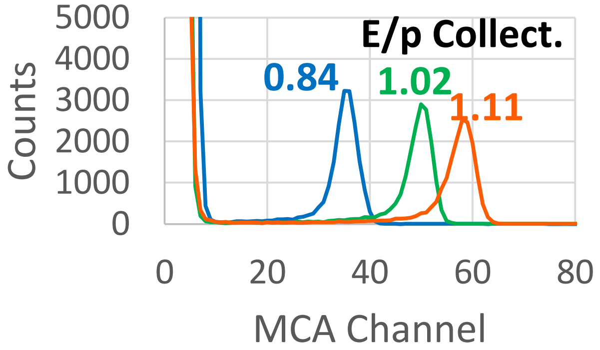

- **R%** improves **with E/p** in the **collect.** slightly **above scintillation threshold**

Experimental Tests with Alpha Particles

Simulation and First Experimental Measurements

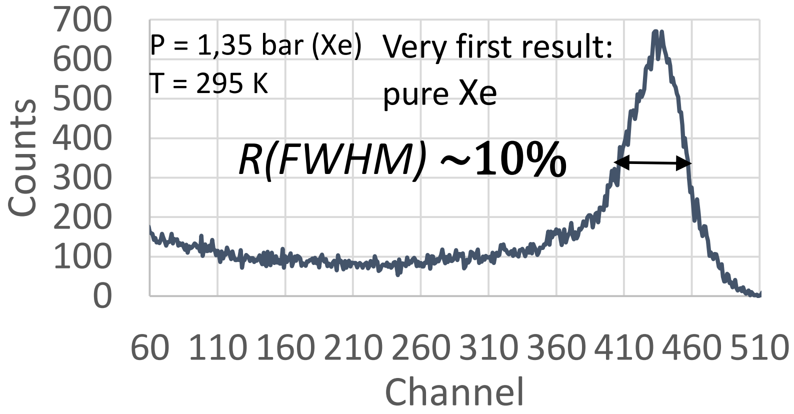

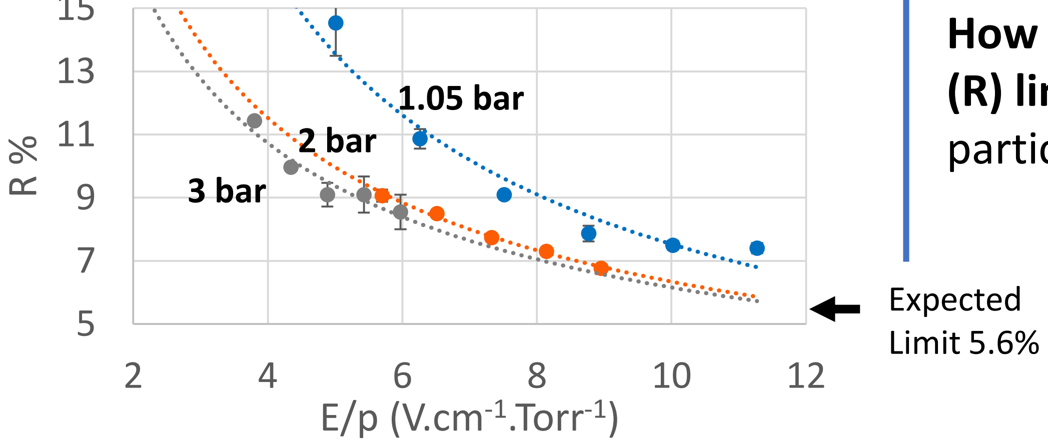

Best R% for alpha particles (experimental)

R = 6.8% (for 4.486 MeV)

We can see a trend towards **R=5.6%**

How far are we **from** the **energy resolution (R) limit** for the detector with alpha particles?

Experimental Tests with Alpha Particles

Simulation and First Experimental Measurements

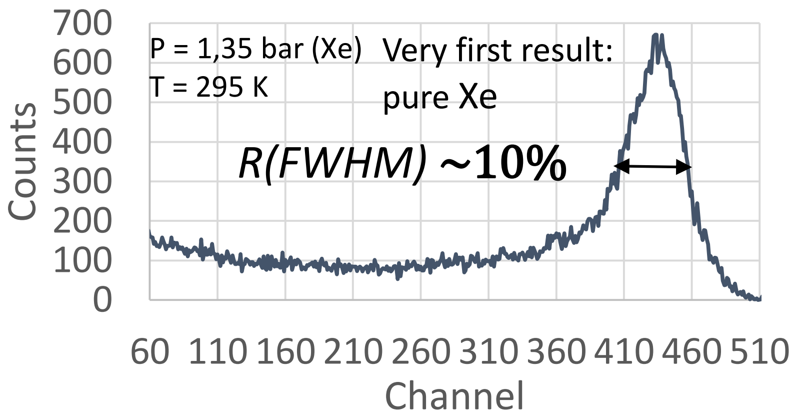

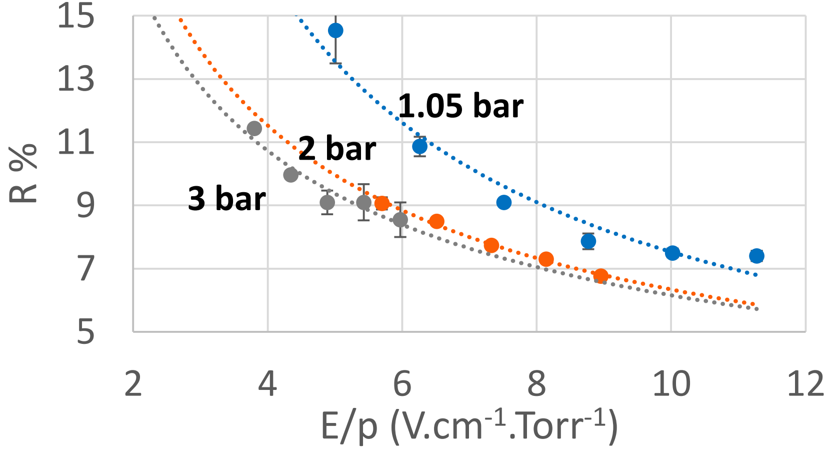

Factors contributing for the Energy Resolution limit

Radiation not monoenergetic

$$R = 2{,}355\sqrt{\underbrace{\frac{F}{\bar{n}}}_{\text{e-}} + \underbrace{\frac{1}{\bar{n}} \times \frac{J}{N_S}}_{\text{ampl.}} + \underbrace{\frac{1}{N_e}\left(1 + \left(\frac{\sigma_q}{G_q}\right)^2\right)}_{\text{photosensor}} + \underbrace{\boxed{\left(\frac{\frac{ENC}{e}}{\bar{n}G}\right)}}_{\text{electronics}} + \underbrace{\boxed{\left(\frac{\sigma_n}{\bar{n}}\right)^2}}_{\text{energy}}}$$

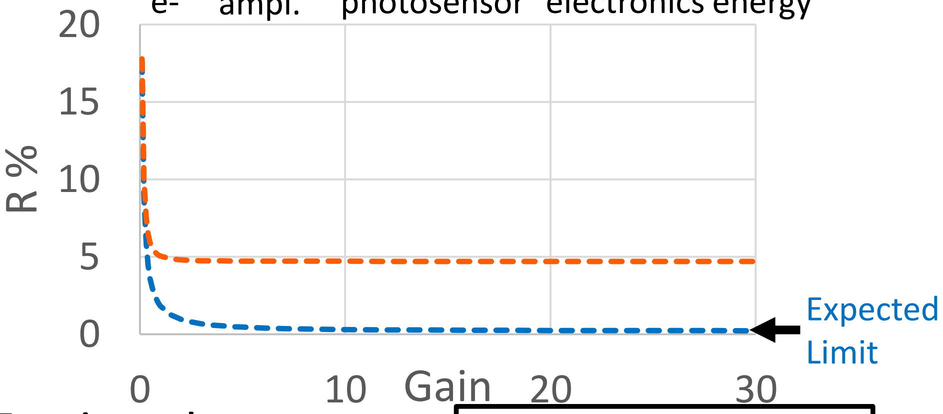

Experimental
R = 6.8% (for 4.486 MeV)
Theor. limits
R = 4.8% (for 4.486 MeV)

Radiation monoenergetic

R = 2.73% (for 662 keV) **G=30**

3.

Conclusion and Future Work

Conclusions and Future Work

We believe that the results of this work demonstrate the feasibility of a new detector based on HPXe GPSC. For the present moment an energy resolution better than **R=6.8%** for **Am241 (alpha-particles)** was achieved in the first measurements.

Main Advantages of this MGHP-GPSC detector:

- Improved solid angle,
- Improved active volume of detection,
- Improved detection efficiency (**20%)** and gain (30 phe-/e-) – pressure dependent,
- Optimized biasing voltage (5x lower than in the previous prototype)

Next step...

- Improve the performance – starting with the associated electronics and solid angle corrections

(more ruggedized, better energy resolution)

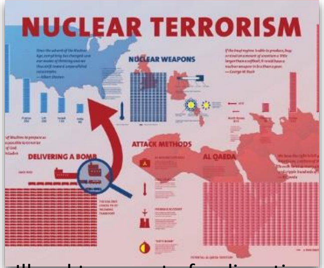

Illegal transport of radioactive material

Homeland Security

Fossil fuel detection

Geological Prospection

X-rays fluorescence analysis

Experimental Physics

Neutron detection applications

Medical Applications

Thank you!

Associazione Frontier Detector for Frontier Physics
Young Researcher Grant

Questions?

REPÚBLICA PORTUGUESA
PD F
FCT PhD PROGRAMMES
Cofinanciado por:
COMPETE 2020
PORTUGAL 2020
UNIÃO EUROPEIA
Fundo Europeu de Desenvolvimento Regional

4.

Spare Slides

The Experimental System

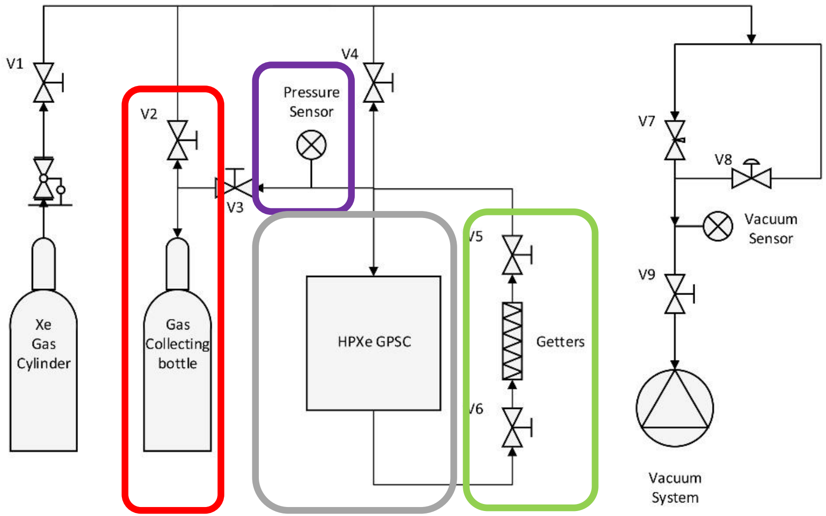

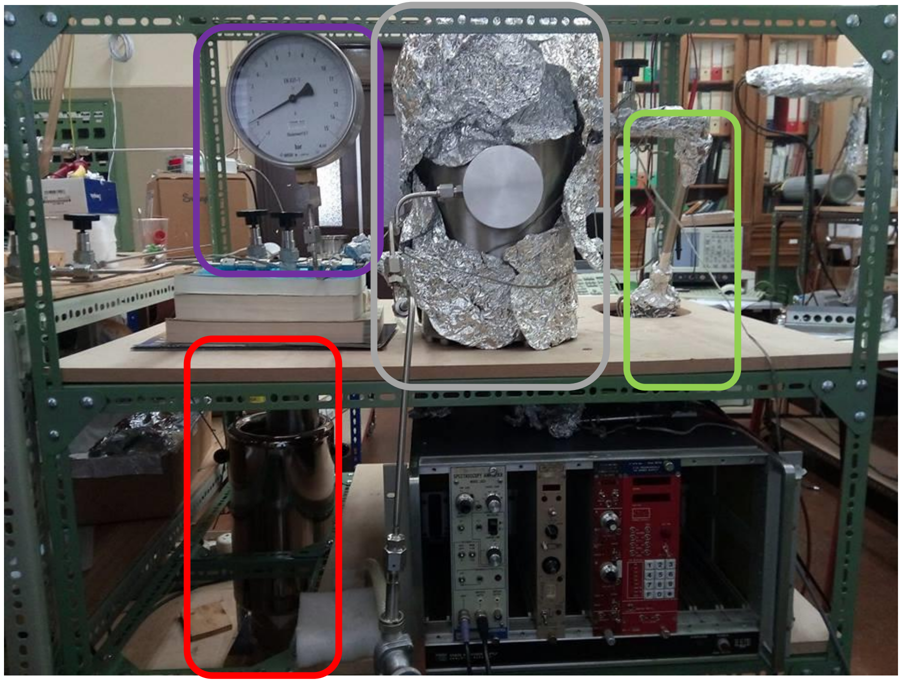

Effects affecting the Scintillation

Solid Angle Effects

$$N_S = \iint \underbrace{(AE_S(r) - pB)}_{\text{Photon production}} \underbrace{\left(\frac{2\pi - 2\theta(r)}{2\pi}\right)}_{\text{Anode shadow}} \underbrace{\frac{\Omega(r,z)}{4\pi}}_{\text{Solid angle}} dr\, dz$$

Solid angle

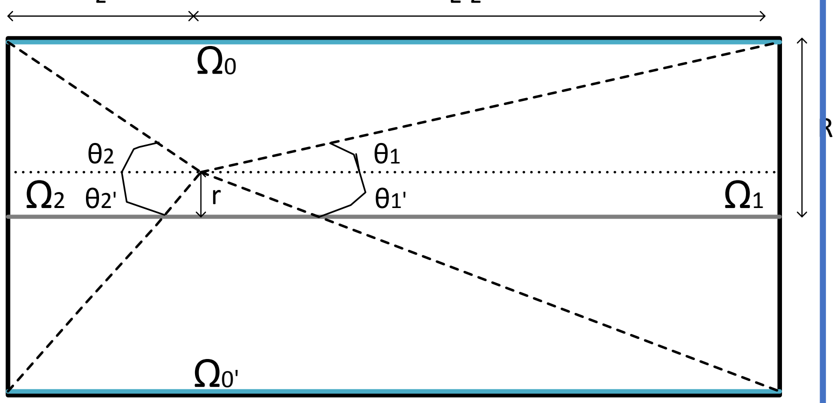

$$\Omega(r,z) = \Omega_0\ (r,z) = 4\pi - \ \Omega_1\ (r,z) - \Omega_2\ (r,z)$$

To simplify we assume that all photons are emitted at the detector axis (r=0). This way we obtain.

$$\Omega_i\ (z) = \int_0^{2\pi}\int_0^{\theta_i} \sin\theta\ d\theta\ d\varphi \qquad \Omega_i\ (z) = 2\pi(1 - cos\ (\theta_i))$$

$$\Omega_0\ (z) = 2\pi(cos\ (\theta_1) + cos\ (\theta_2))$$

$$\Omega(z) = 2\pi\left(\frac{(L-z)}{\sqrt{(L-z)^2+R^2}} + \frac{z}{\sqrt{z^2+R^2}}\right)$$

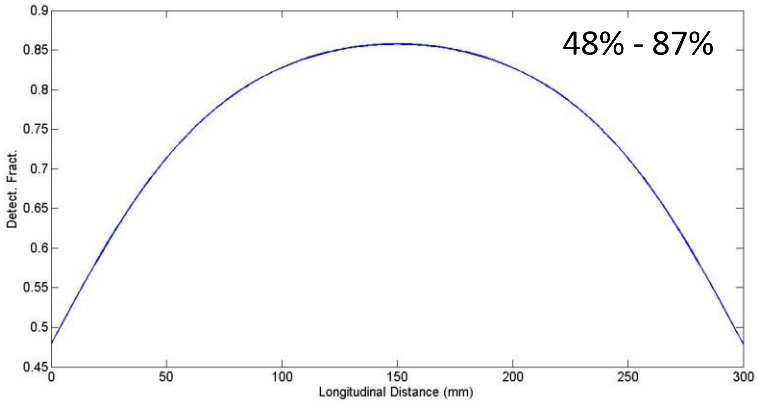

Effects affecting the Scintillation

Anode Shadow

$$N_S = \iint \underbrace{(AE_S(r) - pB)}_{\text{Photon production}} \underbrace{\left(\frac{2\pi - 2\theta(r)}{2\pi}\right)}_{\text{Anode shadow}} \underbrace{\frac{\Omega(r,z)}{4\pi}}_{\text{Solid angle}} dr\, dz$$

Photon production Anode shadow Solid angle

Anode shadow

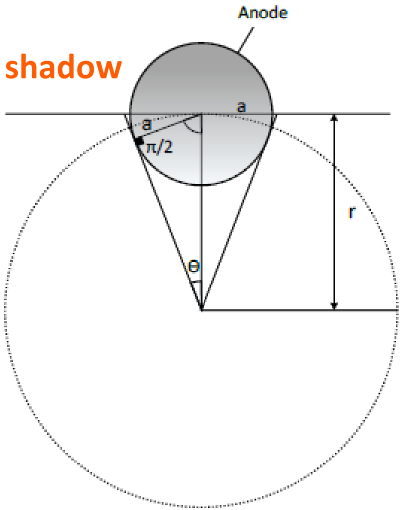

a – anode radius
r – radial position of the emission

$$\eta_a = \left(\frac{2\pi - 2\theta(r)}{2\pi}\right) = \left(\frac{2\pi - 2\sin^{-1}\left(\frac{a}{r}\right)}{2\pi}\right)$$

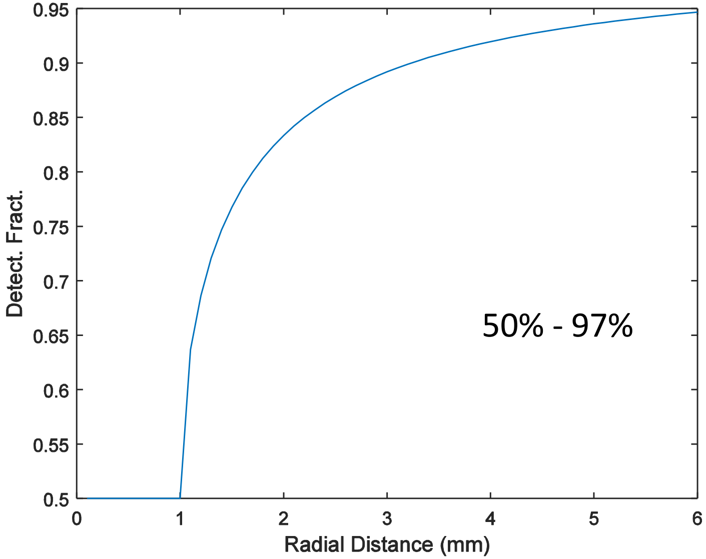

Effects affecting the Scintillation

Extraction Efficiency vs Incidence angle

What do we know so far of CsI as a reflective photocathode?

Cesium iodide (CsI) photocathodes are widely used as VUV photo-sensors (High QE and Stability)

Effective quantum efficiency of the photocathodes is reduced due to photoelectron backscattering at high pressures.

What about the Quantum efficiency dependence on the photon incidence angle at pressures higher than the atmospheric?

Limited Information

Objective

Measure the quantum efficiency of a CsI photocathode in gaseous xenon at different pressures and for different photon incidence angles.

Improve solid angle corrections in large volume gas detectors

Effects affecting the Scintillation

Extraction Efficiency vs Incidence angle

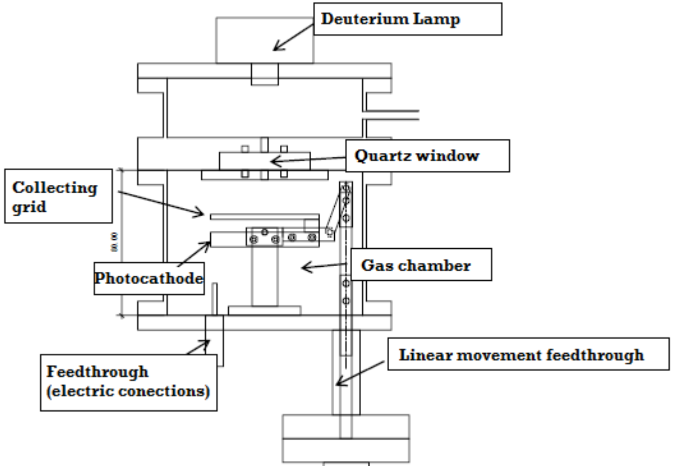

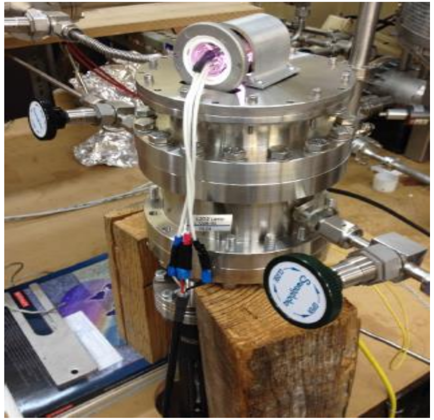

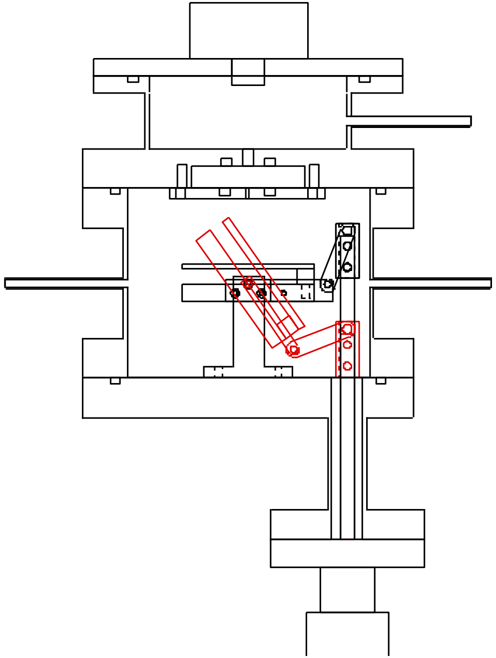

- The collimated photons enter the detector through the quartz window, irradiate the photocathode and the photocurrent induced in the grid is measured using a Keithley 6512 electrometer.

- The photocathode plate is connected to a linear motion feedthrough through a crank, so that the photon incident angle on the photocathode can be varied between 0 and 50 degrees.

Effects affecting the Scintillation

Extraction Efficiency vs Incidence angle

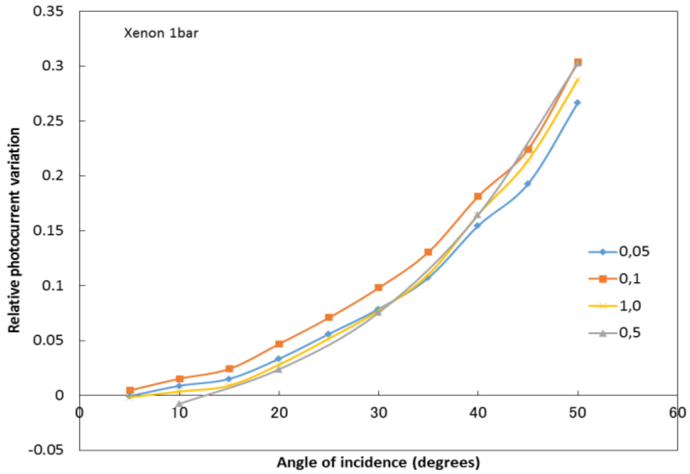

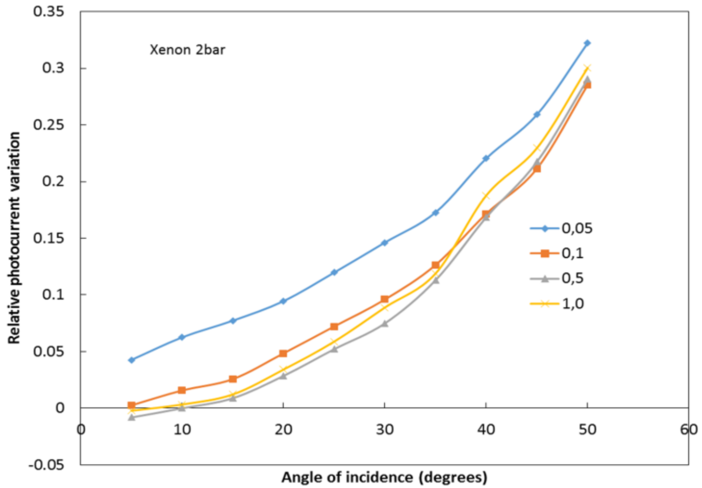

Conclusions:

- Photon incident angle on the photocathode can be varied by introducing the linear motion feedthrough through a crank in the chamber filled with high pressure gases.

- Relative quantum efficiencies of the CsI photocathode as a function of the photon incident angle from 1 bar and up to 5 bar of xenon was measured.

Problems affecting large area detectors
COMPENSATION OF SOLID ANGLE EFFECTS

Existing techniques:

Electron focusing techniques

- Brings the electrons close to the detector axis to maximize the solid angle.

Curved-grid techniques

- Makes use of two grids, the first curved and the second planar, for the definition of the scintillation region in such a way that the electric field increases radially.

Masked-photosensor techniques

- Photosensor is covered with a mask with a light transmission that increases radially, that compensate the decrease in the solid angle.

So far have only been applied to detectors with planar geometry.

Examples

Curved-technique

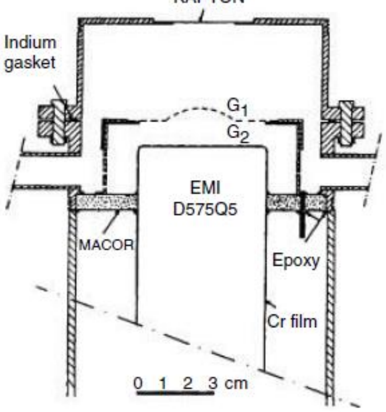

a)

Masked-photosensor

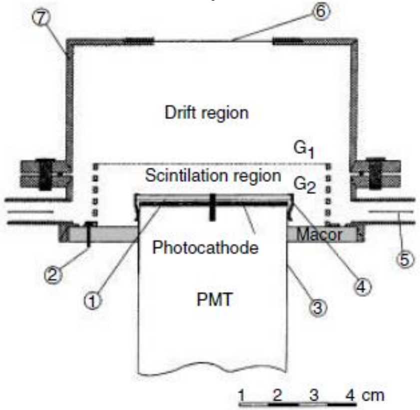

1 - Quartz wafer with grid G2 and mask compensation
2 - G1 feedthrough
3 - Chromium film
4 - Electrical contacts for G2
5 - To gas purifier
6 - Kapton window, 75 μm thick
7 - Stainless steel

b)

[dos Santos 2001] X-Ray Spectrom. 2001; 30: 373-381]

Problems affecting large area detectors
COMPENSATION OF SOLID ANGLE EFFECTS

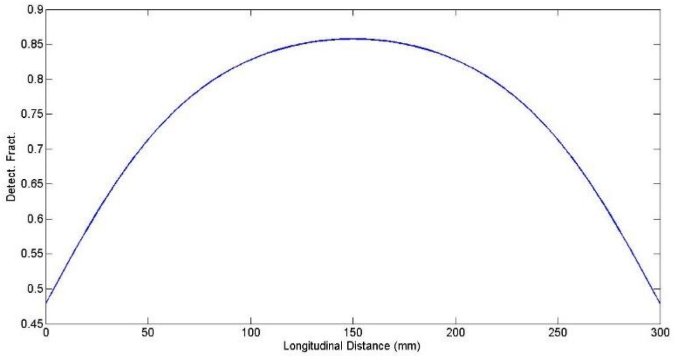

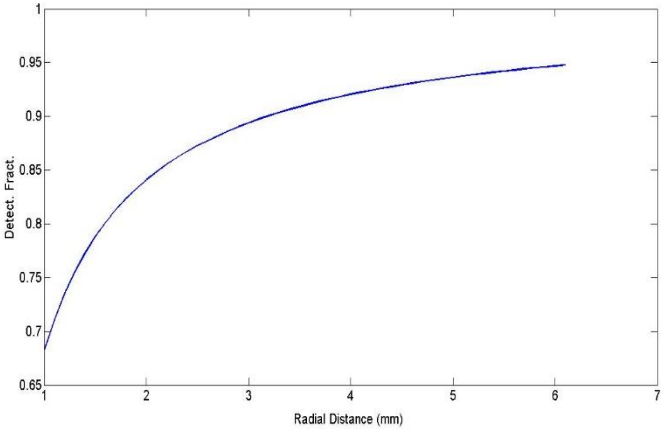

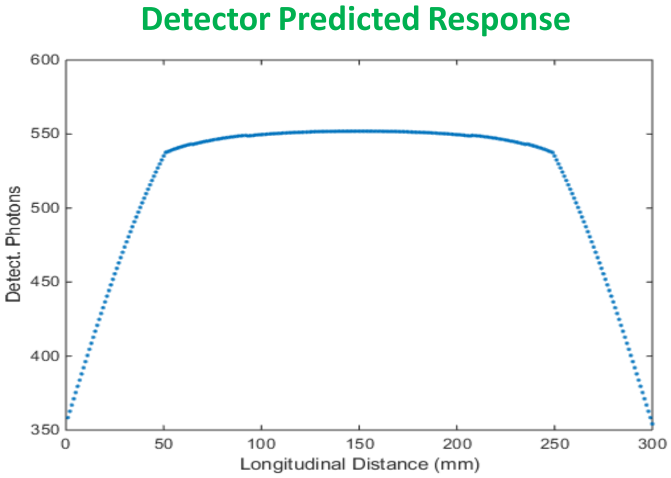

Solid angle compensation can be achieved by modifying E/p.
(Patent to be submitted soon.)

Planar vs Cylindrical Geometry

Considerations on light production

$$\frac{1}{p}\frac{dN_s}{dr} = A\,{}^{E_S}\!/_{p} - B$$

Planar $$\frac{dN_s}{dr} = AE_S - pB$$ **Cylindrical**

Planar:

$$N_S = \int_0^d AE_S - pB\ dr$$

$$N_S = \int_0^d A\frac{\Delta V_p}{d}E_S - pB\ dr$$

$$N_S = A\Delta V_p - pB\mathrm{d}$$

Cylindrical:

$$N_S = \int_a^r AE_S(r) - pB\ dr$$

$$N_S = \int_0^d A\frac{\Delta V_c}{r\log\left({}^{b}\!/_{a}\right)}E_S - pB\ dr$$

$$N_S = A\frac{\Delta V_c \log({}^{r_S}\!/_{a})}{\log({}^{b}\!/_{a})} - pB\Delta\mathrm{r}$$

$$\Delta V_p = \left(\frac{\log\left({}^{r_S}\!/_{a}\right)}{\log\left({}^{b}\!/_{a}\right)}\right)\Delta V_c$$

To obtain the same scintillation output

Considerations on Optical Transmission and Solid angle

Planar	**Cylindrical**
Uses 3 grids	Uses 2 grids
T_{opt}=$\left(T_{grid}\right)^3$	T_{opt}=$\left(T_{grid}\right)^2$
Solid angle	Solid angle
Ω_{planar}=0,14	$\Omega_{cyl.}$=0,7 $(uniform)$
Anode shadow	Anode shadow
η_a=0	η_a=0,50 $(maximum)$

$$Gain = N_S.(1-\eta a).\,T_{opt}\,.\,QE.\,\eta.\Omega$$

$$\boxed{\frac{Gain\ cylind.}{Gain\ planar} = \frac{\Omega_c(1-\eta_a)}{T_{grid}.\Omega_p} \sim 3}$$

Simulation Results

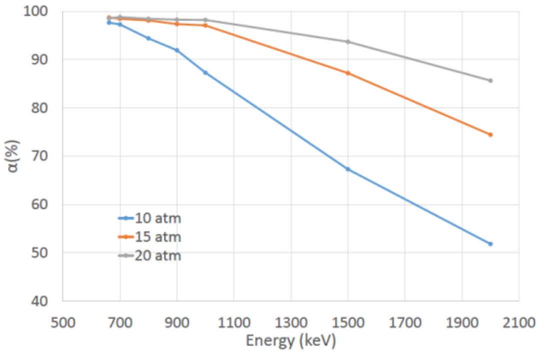

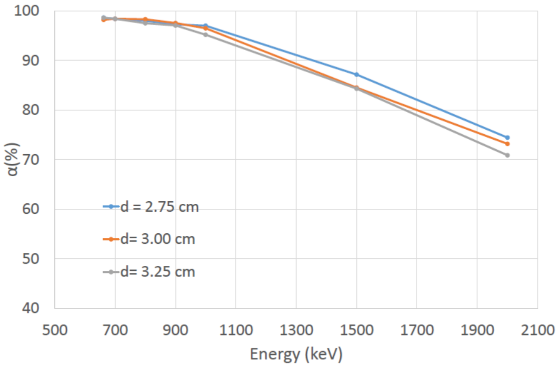

Best results expected for pressures above 15 atm.

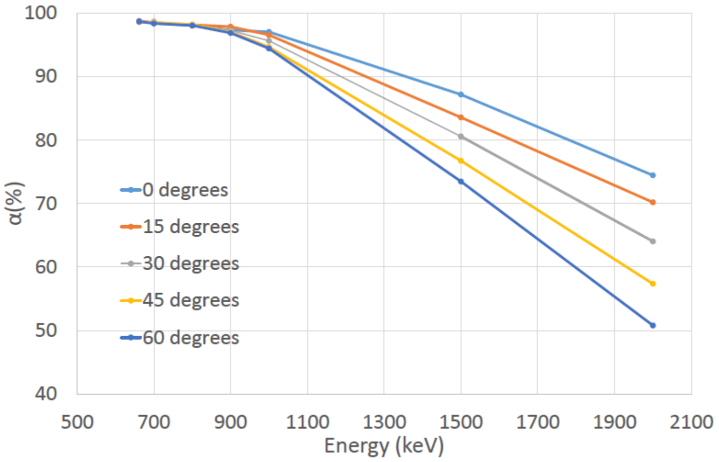

- Good energy absorption efficiency up to 1 MeV.

Almost independent of..

- Emission angle
- Radial emission position